

Supplementary Information for:

Metabolic novelty originating from horizontal gene transfer is essential for leaf beetle survival

Roy Kirsch^{*1}, Yu Okamura¹, Wiebke Haeger^{1, §}, Heiko Vogel¹, Grit Kunert², Yannick Pauchet^{*1}

¹Department of Insect Symbiosis, Max Planck Institute for Chemical Ecology, 07745 Jena, Germany. ²Department of Biochemistry, Max Planck Institute for Chemical Ecology, 07745 Jena, Germany

[§]Present address: Department of Biology, Norwegian University of Science and Technology (NTNU), Trondheim, Norway.

*Corresponding Authors: RK, rkirsch@ice.mpg.de, 0049-3641571555; YP, ypauchet@ice.mpg.de, 0049-3641571507, Hans-Knoell-Str. 8

This PDF file includes:

Supplementary text (Results)

SI References

Figures S1 to S7

Table S1

SUPPLEMENTARY RESULTS

CRISPR/Cas9-mediated knockout of GH28 endo-PGs and characterization of gene copy number variation

Previous characterization of the *P. cochleariae* GH28 proteins revealed GH28-1, -5 and -9 to be endo-PGs hydrolyzing homogalacturonan, the polymeric backbone of pectin (1). Thus, we were aiming to knockout the three corresponding genes using the CRISPR/Cas9 system to eliminate PG activity from the beetle's gut. Since the intron positions of beetle GH28s are highly conserved and known for *P. cochleariae* GH28-2 and GH28-4, we used this information to identify target sites in the middle of their

exons. In order to analyze the impact of impaired PG activity, the three target *GH28* genes were knocked out in a consecutive, two-step manner. Due to the high sequence similarity of *GH28-5* and *GH28-9*, we screened for identical target sites between the two genes to knock them out simultaneously. Three crisper RNAs (crRNAs) targeting functionally important sites in exon1 and exon3 were selected (Fig. 1, Fig. S1; Table S1). Similarly, three crRNAs were selected to specifically target *GH28-1*. The functionality of pre-assembled ribonucleoprotein complexes (RNPs) were tested *in vitro* before egg injections (Fig. S1). In the first step, ~500 eggs were injected with a mixture of the three gRNA/RNPs targeting *GH28-5* and *GH28-9* simultaneously to generate a *GH28-5/28-9* homozygous knockout line.

Genomic DNA from G0 larval individuals was extracted to generate PCR amplicons of *GH28-5* and *GH28-9* exon1 and exon3 for Indel Detection by Amplicon Analysis (IDAA) in default of a visible phenotype indicating mosaicism (Fig. S2A, B). As none of the G0-mosaic individuals was identified to carry a mutation in both *GH28-5* and *GH28-9*, matings with a pool of G0 adults, mosaic in either of the *GH28* gene were set up. The offspring G1 was screened for inherited mutations by IDAA (Fig. S2C) followed by Sanger sequencing of PCR amplicons for IDAA-positive individuals. Whereas further crossings led to *GH28-5* homozygous knockout already in G2, a lack of wild-type signal in case of *GH28-9* IDAA, indicating a *GH28-9* homozygous knockout, was reached first in G4. The difficulty to obtain *GH28-9* homozygous knockout individuals was in line with the detection of up to four different deletions per target site in a single larva by IDAA and sequencing (Fig. S2D). This indicated the presence of an additional *GH28* sharing high sequence similarity with *GH28-9* rather than multiple alleles.

We decided to sequence the genome as well as full-length cDNAs using Oxford Nanopores and PacBio Iso-Seq sequencing methods respectively to further support the presence of an additional, so far overlooked *GH28* gene in *P. cochleariae*. Genome assembly revealed three contigs harboring *GH28-9*, with one contig containing a highly similar additional gene in close proximity to the other *GH28-9* gene (Fig. S3A). Whereas contig_23458 and contig_15494 represent two haplotypes with a *GH28-9* allelic variant each, contig_23457 possesses an additional gene (*GH28-10*). This copy number variation (cnv) between individuals occurs in the same genomic environment, confirmed by the presence of identical flanking genes. In addition, we mapped the coding sequences of the *GH28s* as well as the flanking genes back to the Oxford Nanopore raw reads to exclude the possibility of assembly artefacts (Fig. S3B). This mapping approach clearly shows the presence of both *GH28-9* and *GH28-9 + GH28-10* reads. RNA Iso-Seq further confirmed the additional *GH28-10* gene as well as its transcriptional activity. The multiple amino acid alignment of the corresponding *GH28-9* and *GH28-10* proteins derived from the genome assembly and the RNA Iso-Seq data highlights the high sequence similarity between the deduced amino acid sequences that can be discriminated only in 13 amino acid positions (Fig. S3C). Taken together, our *P. cochleariae* wild-type lab culture was found to contain a *GH28* cnv between individuals, either possessing nine or ten *GH28* genes. In contrast, we found no evidence of cnv for

any other *GH28*. To obtain data on the frequency of the *GH28-10* gene in our wild-type lab culture, we designed diagnostic primers spanning intron 3 that possesses a length polymorphism comparing *GH28-9* and *GH28-10* genes (Fig. S3D). Representative PCR products were cloned and sequenced verifying the lowest band (~ 1300 bp) to exclusively correspond to *GH28-10* whereas all the bands above correspond to *GH28-9* indicating allelic variability for this gene (Fig. S3E). A screening of ~ 100 wild-type beetles first, revealed about 97% of individuals possessing the *GH28-10* gene and secondly confirmed allelic variation for *GH28-9* in our beetle population (Fig. S3F).

At this stage we already obtained a triple mutant and found *GH28-10* is very common in our wild-type culture. Furthermore, our reinvestigation of the *P. cochleariae* *GH28s* confirmed the endo-PG activity of *GH28-10*. In addition, the breakdown products of *GH28-9* and *GH28-10* are highly similar, indicating a benefit for the beetle through increased expression/ enzyme levels (i.e. gene dosage effect). However, when comparing *GH28-9/10* to *GH28-1* and *GH28-5*, breakdown products slightly differ indicating synergistic effects (Fig. S3G-J). Taking the enzymatic activity and widespread presence of *GH28-10* into account, we decided to use the eggs of the *GH28-5/28-9/28-10* knockout line for the subsequent knockout of *GH28-1*. Approximately 100 eggs were injected to finally obtain a quadruple knockout line. Since the screen of G0 individuals revealed a larva with a large deletion mutation in exon3, the subsequent analysis of inheritance and homozygosity after further crossings was possible simply by agarose gel electrophoresis of the PCR amplicons (Fig. S4A).

Mutations were finally confirmed by Sanger sequencing of *GH28-1*, *GH28-5* and *GH28-9* PCR amplicons of 24 individuals from the complete knockout line. By this we not only verified the simultaneous, homozygous knockout of the three endo-PG coding genes targeted initially (Fig. S4A-D) but also confirmed the knockout of the newly identified endo-PG coding *GH28-10* (Fig. 1, Fig. S4C, D). In order to get additional confidence in the mutant genotypes, we sequenced the genomes of the triple and quadruple knockout line and analyzed the target gene environment for unintended long deletions. Previous studies in mammals revealed such long non-homologous end joining deletions that cannot be detected by amplicon sequencing as primer binding sites would be deleted (2, 3). Dot plot and gene synteny plot analyses revealed no such long deletions in the alleles fixed in our knockout lines (Fig. S4E-H).

References:

1. Kirsch R, et al. (2014) Horizontal gene transfer and functional diversification of plant cell wall degrading polygalacturonases: Key events in the evolution of herbivory in beetles. *Insect Biochem Mol Biol* 52:33-50.
2. Kosicki M, Tomberg K, & Bradley A (2018) Repair of double-strand breaks induced by CRISPR-Cas9 leads to large deletions and complex rearrangements. *Nature biotechnology* 36(8):765-771.
3. Shin HY, et al. (2017) CRISPR/Cas9 targeting events cause complex deletions and insertions at 17 sites in the mouse genome. *Nat Commun* 8:15464.



Figure S1 Multiple nucleotide alignment of *P. cochleariae* GH28 coding sequences. GH28-1 to GH28-9 sequences were published previously (HE962193.1 to HE962201.1). The bottom three sequences are the ones from this study. Target sites are located in exon1 (E1) and exon3 (E3), were selected based on the previously published GH28 sequences and are indicated in cyan for GH28-1 and blue for GH28-5, 9, 10, respectively. PAM sites are shown in dark-red and mismatches in target sites are highlighted in orange. Functionality of sgRNAs was tested *in vitro* before injection exemplarily shown for the digestion of the full-length PCR product of GH28-1 by either the individual sgRNAs 3a, 3b and 3c or a mixture of them (agarose gel picture).

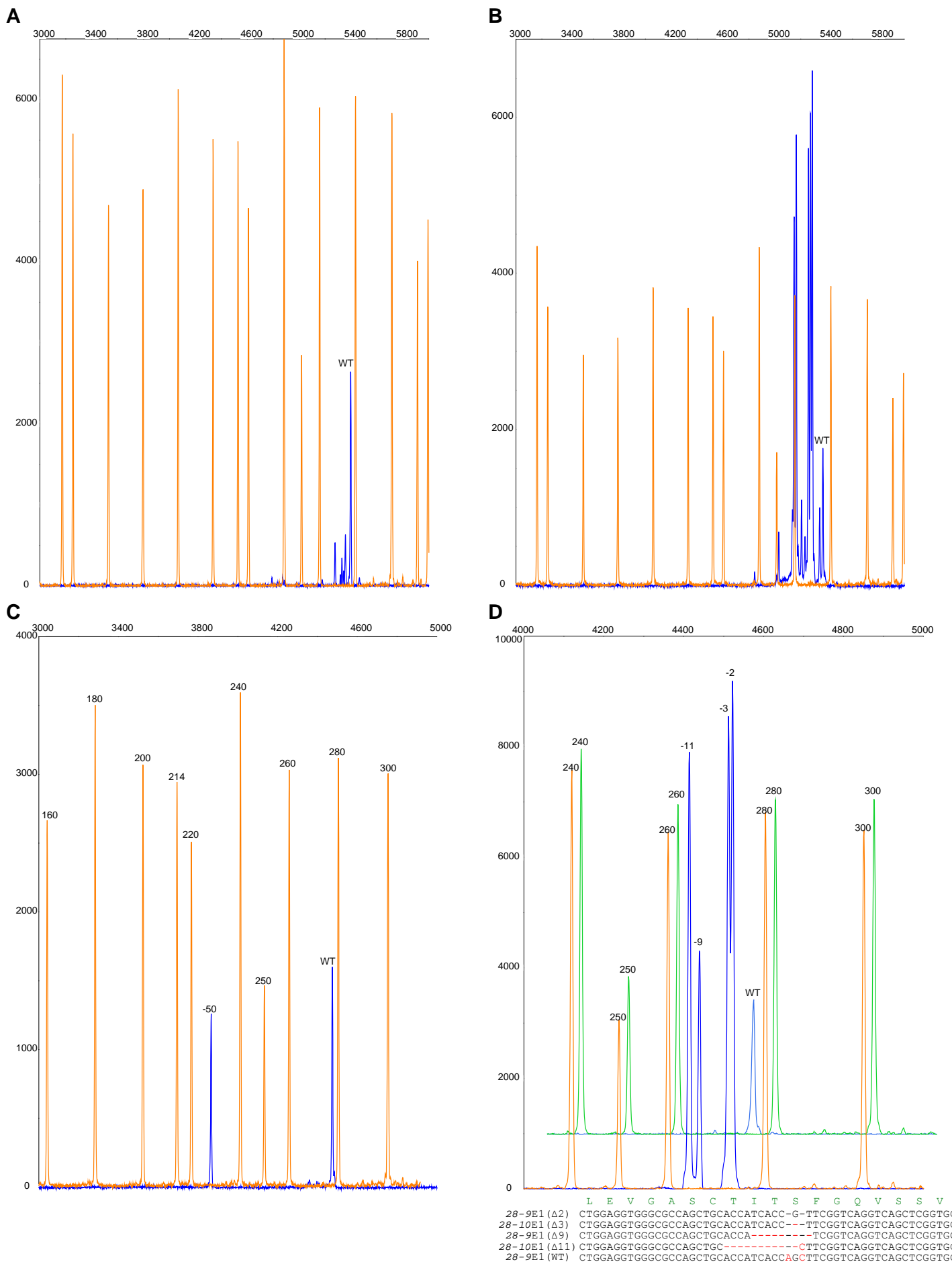
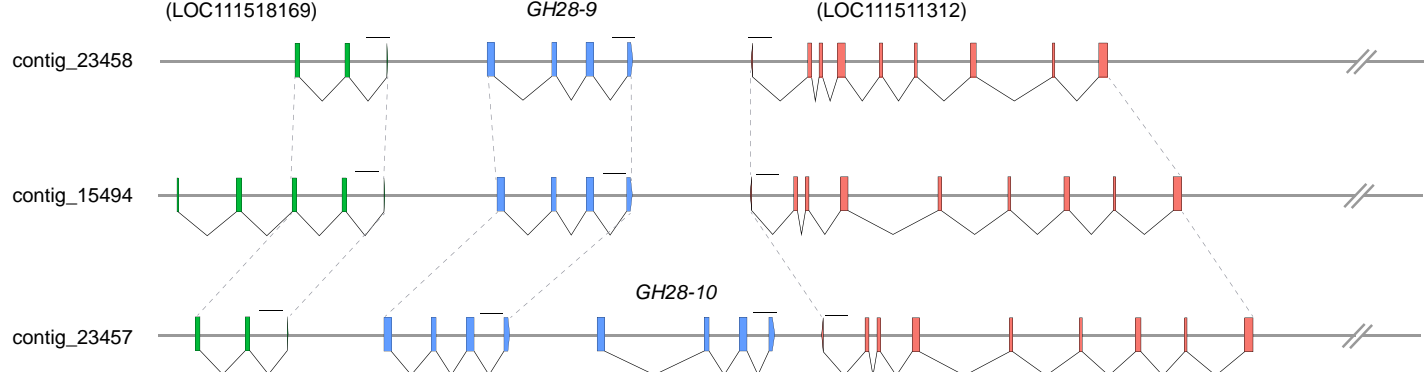


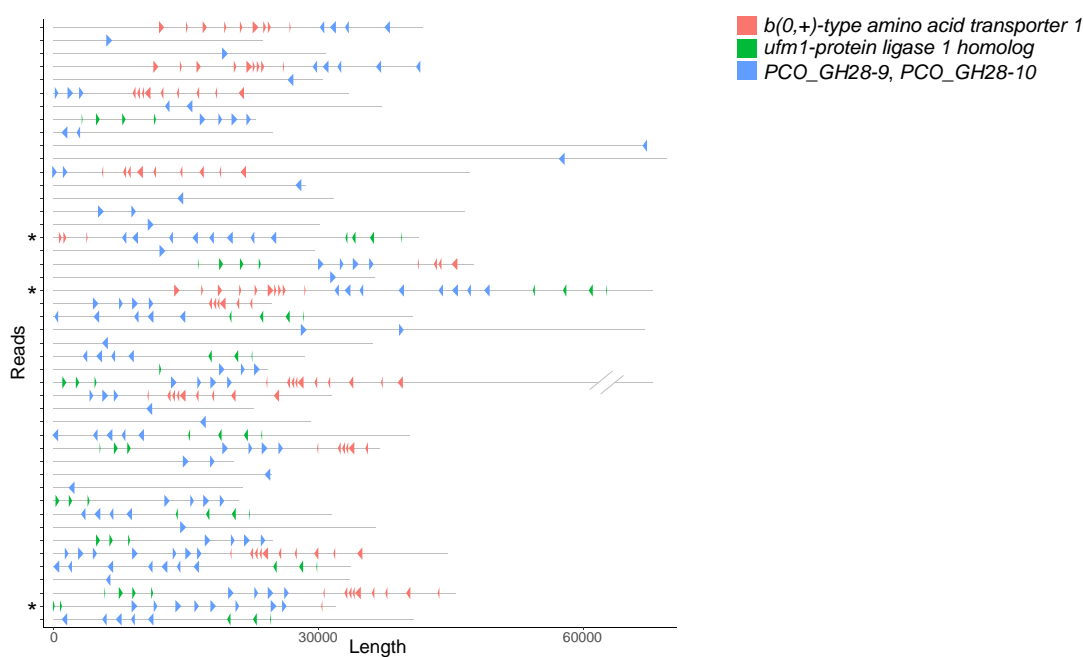
Figure S2 Indel Detection by Amplicon Analysis (IDAA) is shown by electropherograms. Each electropherogram represents the results obtained from a single specimen. Run time in seconds is indicated on the x-axis and signal intensity on the y-axis. G0 individuals were screened for mosaicism in all targeted loci shown exemplarily for A) GH28-5 exon3 and B) GH28-9 exon3. G1 individuals were screened for inherited mutations shown for C) GH28-5 exon3. The detection of four different deletions in G4 individuals for GH28-9/10 exon1 is shown in D). Wild type length of GH28-9/10 exon1 (WT) is shown in a separate peak profile. Sequencing results and sequence assignment to either GH28-9 or GH28-10 are indicated below the electropherogram. Blue peaks indicate PCR amplicons and numbers of deleted nucleotides as well as wild-type peaks (WT) are indicated. The GSLIz600 standard peaks are shown in orange (A-D) and green (D), respectively and corresponding numbers of nucleotides are indicated.

A

Leptinotarsa decemlineata
ufm1-protein ligase 1 homolog
(LOC111518169)

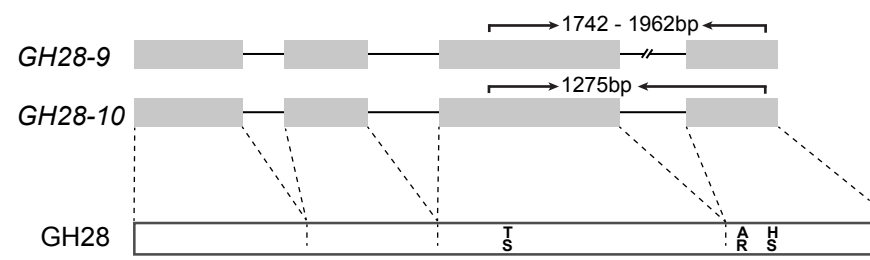
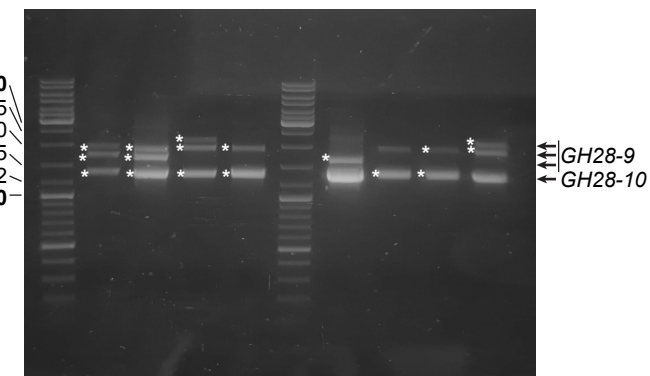
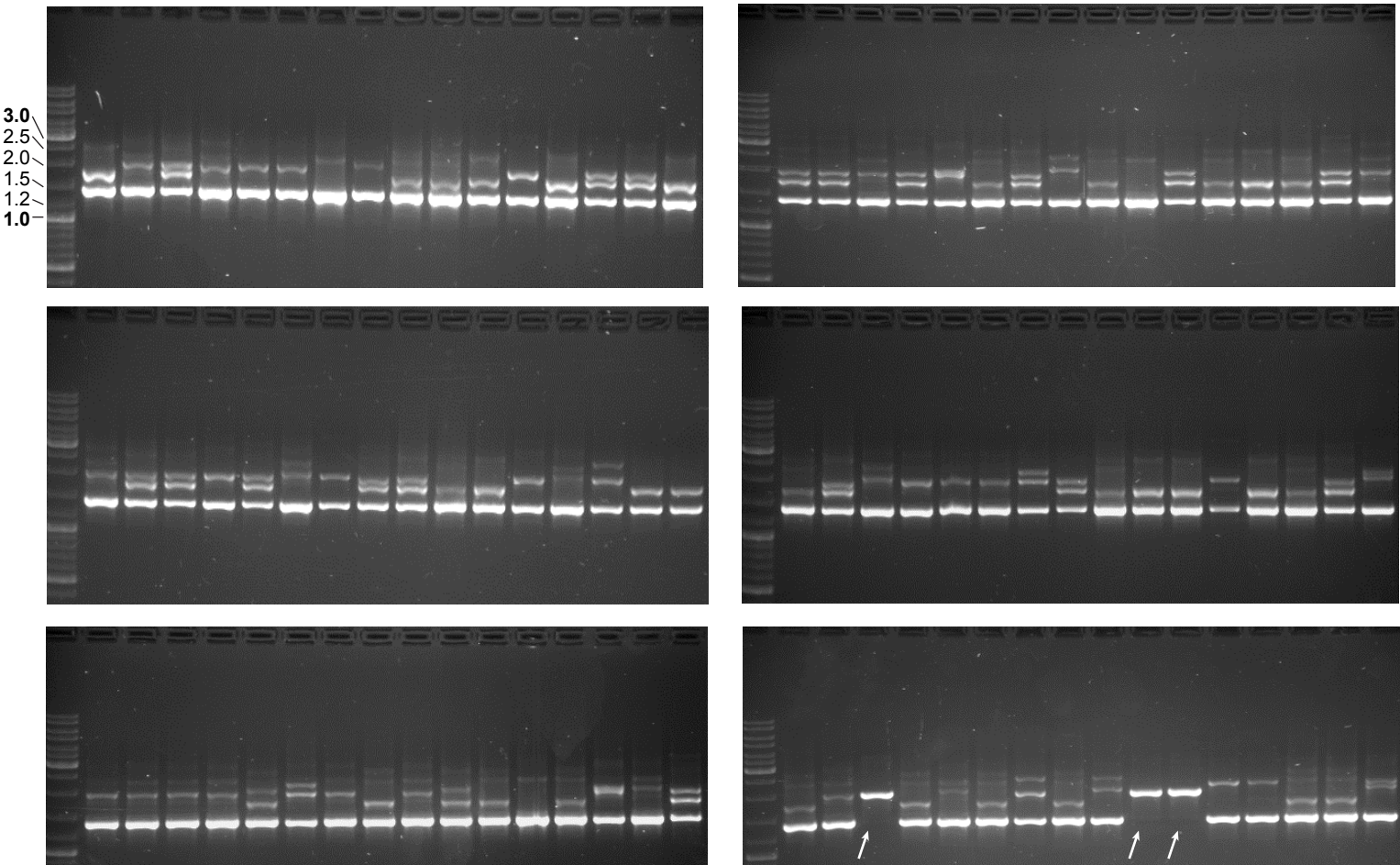


B



C

PCO_GH28-9	1 MFSVKLAFVIAAVYAAASAFPANELEVGA PCO_GH28-9_contig_23458	1 MFSVKLAFVIAAVYAAASAFPANELEVGA PCO_GH28-9_contig_15494	1 MFSVKLAFVIAAVYAAASAFPANELEVGA PCO_GH28-9_contig_23457	1 MFSVKLAFVIAAVYAAASAFPANELEVGA Pco_HQ_transcript12018	1 MFSVKLAFVIAAVYAAASAFPANELEVGA Pco_HQ_transcript7296	1 MFSVKLAFVIAAVYAAASAFPANELEVGA Pco_HQ_transcript6257	1 MFSVKLAFVIAAVYAAASAFPANELEVGA Pco_HQ_transcript10768	1 MFSVKLAFVIAAVYAAASAFPANELEVGA Pco_HQ_transcript10701	1 MFSVKLAFVIAAVYAAASAFPANELEVGA Pco_HQ_transcript282	1 MFSVKLAFVIAAVYAAASAFPANELEVGA Pco_HQ_transcript12518	1 MFSVKLAFVIAAVYAAASAFPANELEVGA PCO_GH28-10_contig_23457	1 MFSVKLAFVIAAVYAAASAFPANELEVGA Pco_HQ_transcript11614
PCO_GH28-9	VKKPKFVKVRATGGSVLTGHLVNLCPQC PCO_GH28-9_contig_23458	VKKPKFVKVRATGGSVLTGHLVNLCPQC PCO_GH28-9_contig_15494	VKKPKFVKVRATGGSVLTGHLVNLCPQC PCO_GH28-9_contig_23457	VKKPKFVKVRATGGSVLTGHLVNLCPQC Pco_HQ_transcript12018	VKKPKFVKVRATGGSVLTGHLVNLCPQC Pco_HQ_transcript7296	VKKPKFVKVRATGGSVLTGHLVNLCPQC Pco_HQ_transcript6257	VKKPKFVKVRATGGSVLTGHLVNLCPQC Pco_HQ_transcript10768	VKKPKFVKVRATGGSVLTGHLVNLCPQC Pco_HQ_transcript10701	VKKPKFVKVRATGGSVLTGHLVNLCPQC Pco_HQ_transcript282	VKKPKFVKVRATGGSVLTGHLVNLCPQC PCO_GH28-10_contig_23457	VKKPKFVKVRATGGSVLTGHLVNLCPQC Pco_HQ_transcript11614	
PCO_GH28-9	HFSDCTVNSNDGNIHKTHSDGGPVID PCO_GH28-9_contig_23458	HFSDCTVNSNDGNIHKTHSDGGPVID PCO_GH28-9_contig_15494	HFSDCTVNSNDGNIHKTHSDGGPVID PCO_GH28-9_contig_23457	HFSDCTVNSNDGNIHKTHSDGGPVID Pco_HQ_transcript12018	HFSDCTVNSNDGNIHKTHSDGGPVID Pco_HQ_transcript7296	HFSDCTVNSNDGNIHKTHSDGGPVID Pco_HQ_transcript6257	HFSDCTVNSNDGNIHKTHSDGGPVID Pco_HQ_transcript10768	HFSDCTVNSNDGNIHKTHSDGGPVID Pco_HQ_transcript10701	HFSDCTVNSNDGNIHKTHSDGGPVID Pco_HQ_transcript282	HFSDCTVNSNDGNIHKTHSDGGPVID PCO_GH28-10_contig_23457	HFSDCTVNSNDGNIHKTHSDGGPVID Pco_HQ_transcript11614	
PCO_GH28-9	HFSDCTVNSNDGNIHKTHSDGGPVID PCO_GH28-9_contig_23458	HFSDCTVNSNDGNIHKTHSDGGPVID PCO_GH28-9_contig_15494	HFSDCTVNSNDGNIHKTHSDGGPVID PCO_GH28-9_contig_23457	HFSDCTVNSNDGNIHKTHSDGGPVID Pco_HQ_transcript12018	HFSDCTVNSNDGNIHKTHSDGGPVID Pco_HQ_transcript7296	HFSDCTVNSNDGNIHKTHSDGGPVID Pco_HQ_transcript6257	HFSDCTVNSNDGNIHKTHSDGGPVID Pco_HQ_transcript10768	HFSDCTVNSNDGNIHKTHSDGGPVID Pco_HQ_transcript10701	HFSDCTVNSNDGNIHKTHSDGGPVID Pco_HQ_transcript282	HFSDCTVNSNDGNIHKTHSDGGPVID PCO_GH28-10_contig_23457	HFSDCTVNSNDGNIHKTHSDGGPVID Pco_HQ_transcript11614	

D**E****F**

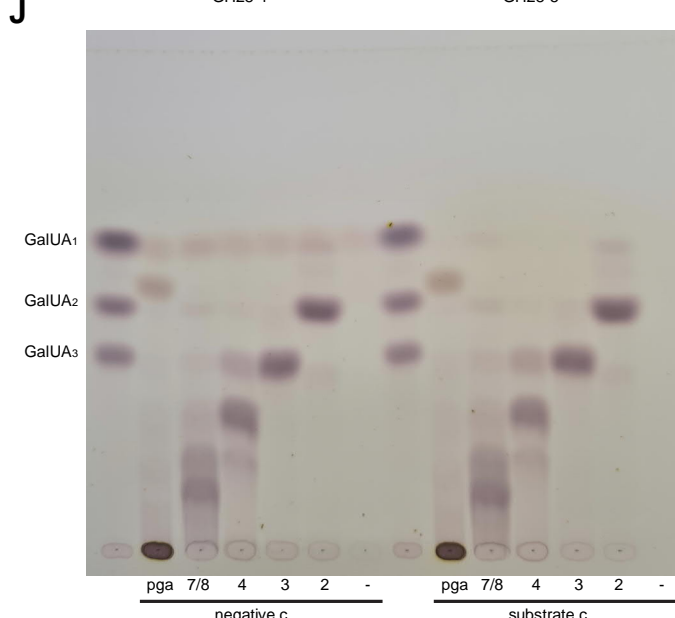
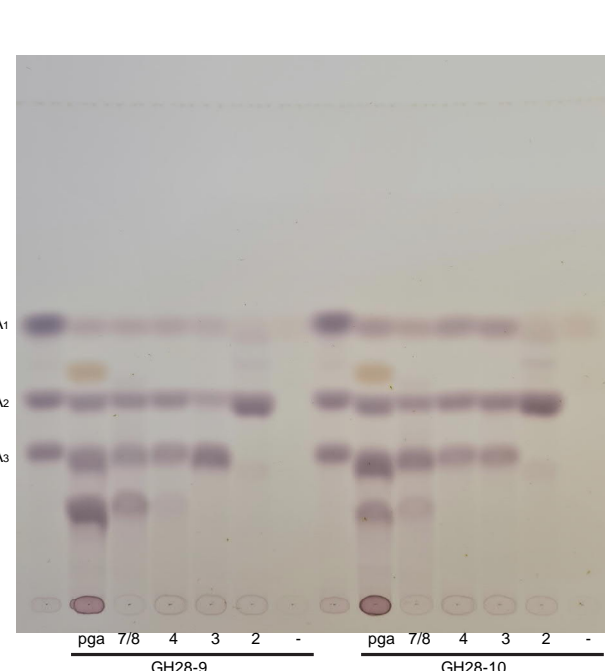
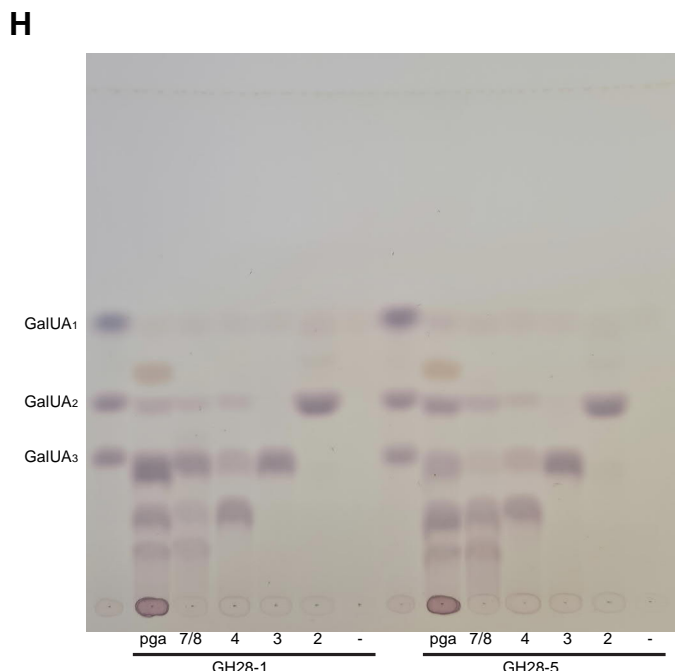
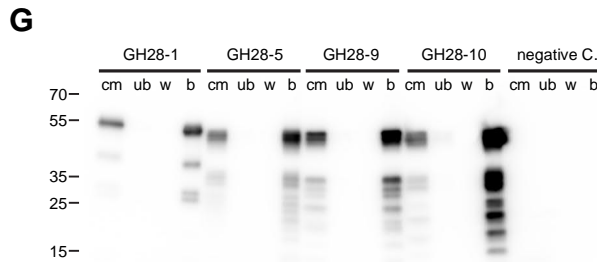
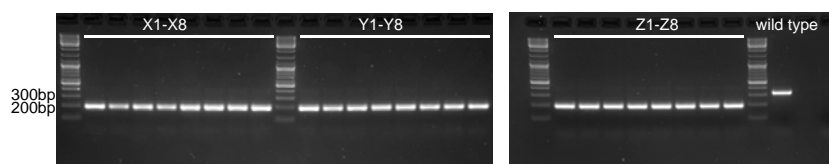


Figure S3 *GH28* copy number variation, haplotype frequency and functional characterization of the recent *GH28-10* copy in our *P. cochleariae* wild-type population.

(A) Genome assembly generated from genomic DNA pooled from three individuals revealed three contigs with a *GH28-9*. Unlike in contig_23458 and contig_15494, in contig_23457 not only *GH28-9* but also an additional *GH28* (*GH28-10*) was found. Flanking genes were shown to be identical and their names refer to homologs in *Leptinotarsa decemlineata*. Bars above each gene represent 1000 nt. (B) Mapping the coding sequences of both *GH28* genes and flanking genes back to the raw reads confirmed *GH28* copy number variation. Asterisks indicate raw reads with *GH28-9* and *GH28-10*. (C) Multiple amino acid alignment of *GH28-9* and *GH28-10* sequences derived from RNA ISO-SEQ of RNA pooled from 10 individuals. Amino acid residues highlighted in blue are discriminating between the two *GH28* genes but those highlighted in grey are not. This confirms both genes to be transcribed in the beetle. PCO_GH28-9 corresponds to the published sequence (CCJ09449.1). (D) The exon-intron structure of the PG encoding genes *GH28-9* and *GH28-10* as well as a corresponding primary structure of a consensus *GH28* protein are shown schematically. Binding sites of PCR primers to discriminate both genes based on length variability of the third intron are indicated with arrows and the estimated length of PCR products based on the genome assembly are written. Discriminative amino acids are highlighted below. (E) Agarose gel-based separation of PCR products using genomic DNA from eight wild-type individuals and primers indicated in panel D. Bands indicated by asterisks were characterized by sequencing and their assignment to *GH28-9* and *GH28-10* respectively is shown next to the gel. (F) Large-scale screening of wild-type population revealed only three out of 96 individuals to lack *GH28-10* indicated by the absence of the corresponding band (arrows). (G) Western blot verifying the heterologous expression and anti-V5 bead-based purification of the endo-PGs *GH28-1*, *5*, *9* including the uncharacterized *GH28-10*. Culture medium of the Sf9 cells (cm), bead-unbound fraction (ub), bead-wash fraction (w) and bead-bound fraction (b) were analyzed. A negative control of non-transfected Sf9 cells was included. (H-J) Heterologously expressed proteins were tested for their pectolytic activity towards different substrates including the polymer polygalacturonic acid (pga) and oligomers ranging from octamer to dimer. “-” corresponds to the enzyme-only control. Hydrolysis products were separated by thin-layer chromatography along with the monomer to trimer galacturonic acid standard (GalUA1 to GalUA3). (J) The negative control (from non-transfected Sf9 cells) as well as the substrate control (substrate-only) were included.



28-5/9E1 target

C continued

I S N X V V K N Q D D C V A V N K A Q H V T I S K L O C S G G H G L L S L S V G M S K S K A D N T V S D

D continued

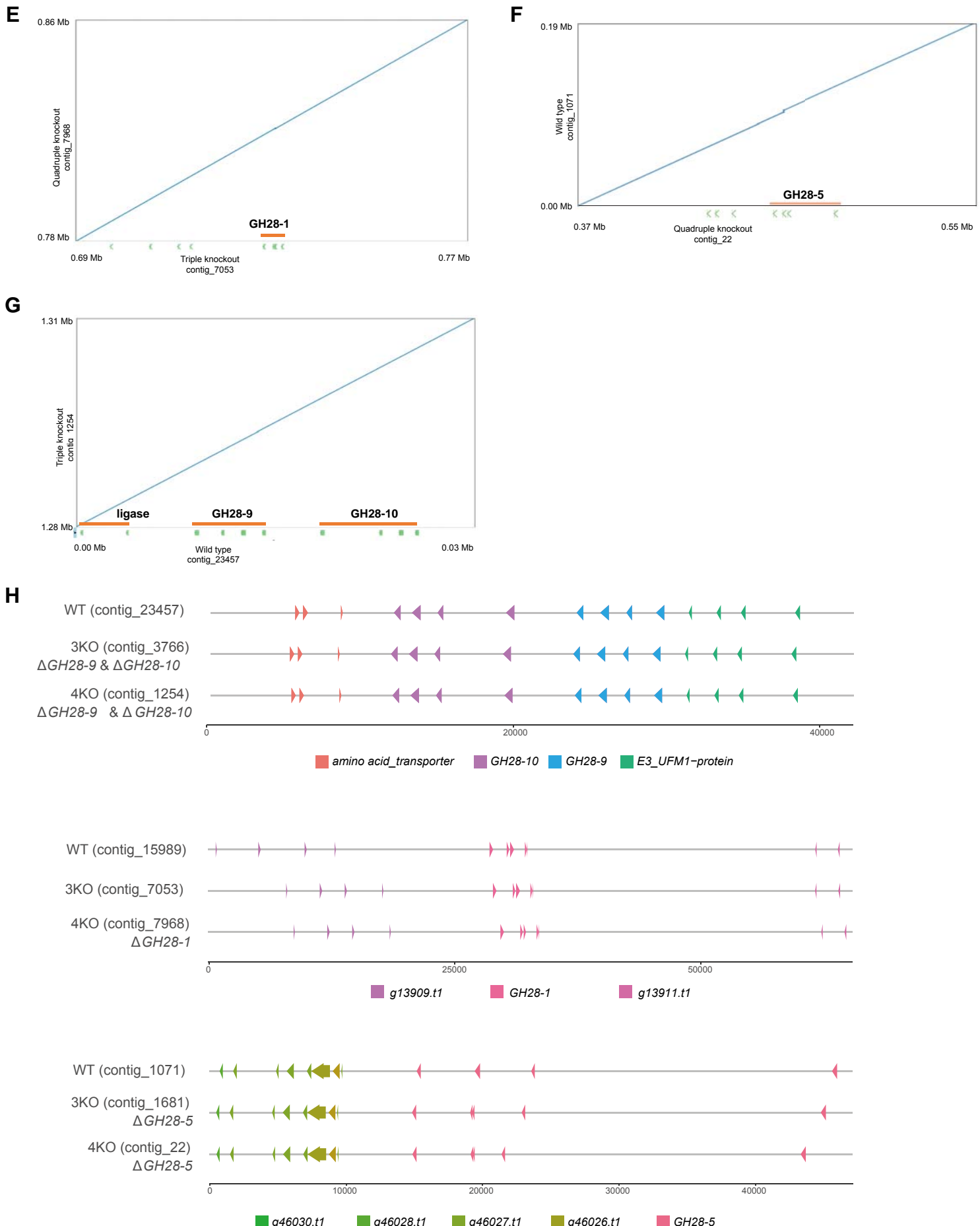


Figure S4 Mutant genotype analysis by either (A-D) multiple nucleotide alignments of *P. cochleariae* GH28 amplicons (quadruple mutant) spanning target sites or (E-H) pairwise comparison of genomic regions flanking target sites.

(A-D) PCR products from 24 individuals (X1 to Z8) were cloned and multiple colonies of each genomic region and individual were sequenced. In case of GH28-1 only colonies from eight individuals were sequenced as the size of the deletion allowed for further verification of the mutation by agarose gel electrophoresis (A bottom). Results verify the consistency of mutations for the loci (A) GH28-1, (B) GH28-5, (C) GH28-9 and 10 exon1 and (D) GH28-9 and 10 exon3. A difference between deletions in GH28-9 and 10 is obvious. sgRNA target sites as well as translated ORFs of the wild-type sequence are highlighted on top of each alignment.

(E-G) Dot plots illustrating the high sequence similarity of genomic regions containing target GH28 genes comparing wild type, triple knockout and quadruple knockout contigs from respective genome assemblies. (H) Synteny plots of the same genomic regions illustrating conserved flanking genes of target GH28 genes comparing wild type, triple knockout and quadruple knockout contigs. These analysis exclude large, unintended deletions.

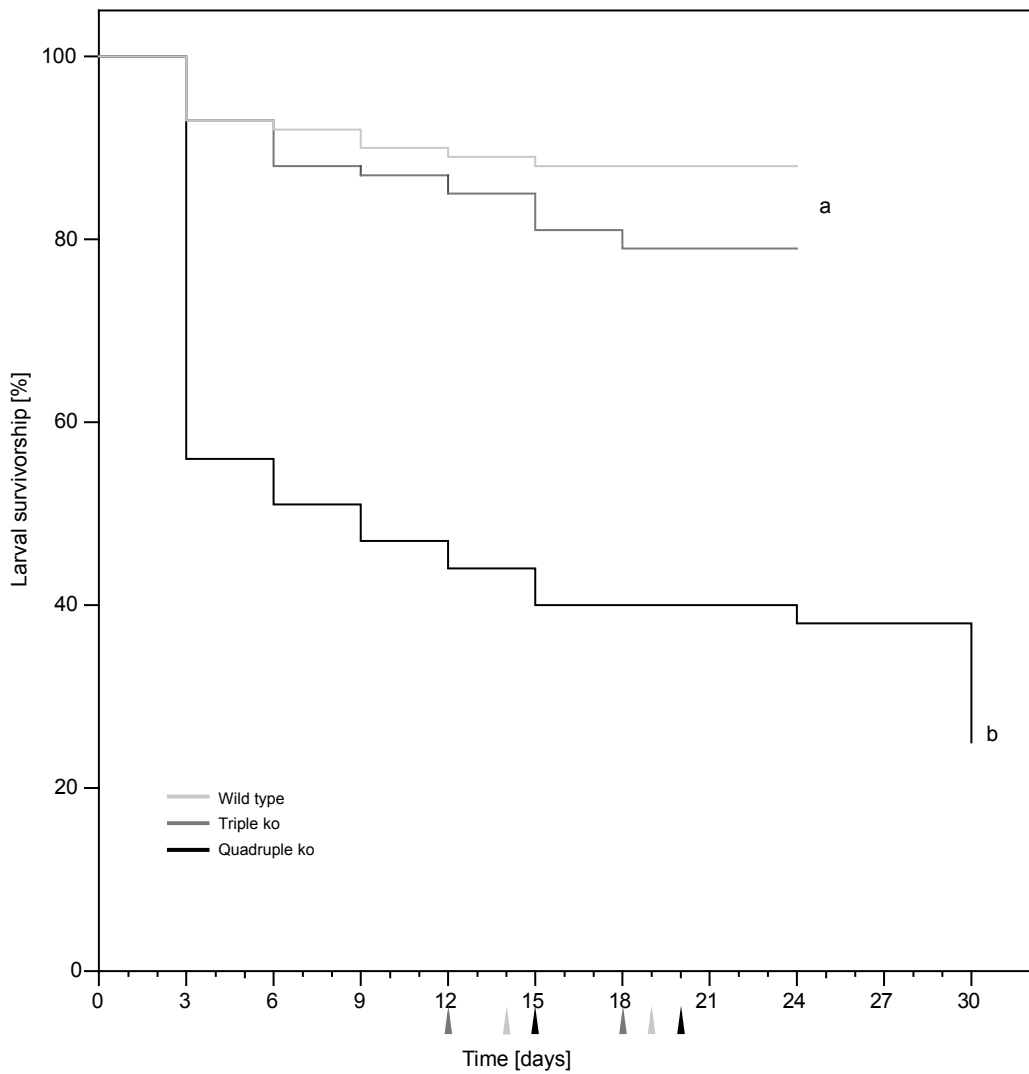


Figure S5 Fitness differences between wild-type (light grey), triple ko (dark grey) and quadruple ko (black) population fed with mature Chinese cabbage leaves from supermarket (standard rearing conditions). Kaplan–Meier survivorship curves of *P. cochleariae* (1st instar larvae to adult eclosion). Arrowheads on the x-axis indicate the beginning of pupation and adult eclosion, respectively. Letters indicate significant differences between populations ($n=100$, $P<0.001$; Log-Rank Survival Test, $\chi^2 = 113.476$).

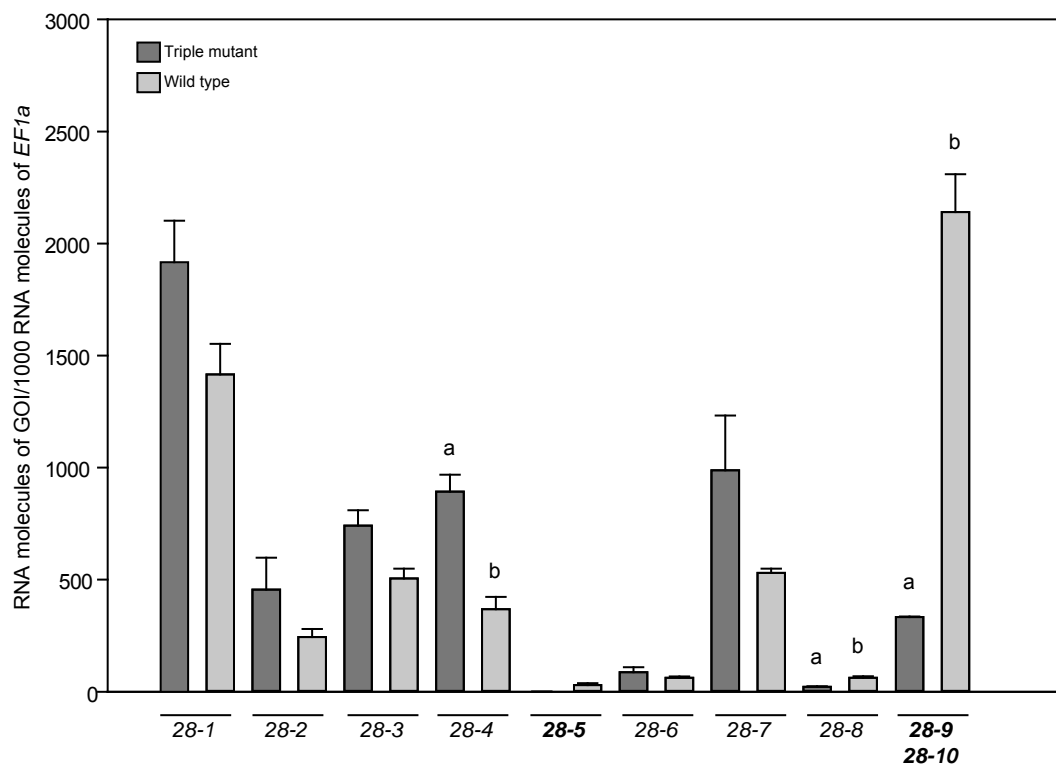


Figure S6 Comparative analysis of GH28 transcript levels between wild-type (light grey) and triple mutant (dark grey) line fed with mature Chinese cabbage leaves from supermarket (standard rearing conditions). Different letters indicate significant differences between lines (for details see table below).

Transcript abundances of GH28 family members are expressed as RNA molecules of gene of interest (GOI) per 1000 RNA molecules of the reference gene *elongation factor 1a* (*EF1a*). Targeted genes in the triple mutant line are highlighted in bold. Signal corresponding to 28-9/28-10 transcripts in the triple mutant was assigned to $\Delta 9/\Delta 12$ 28-9 by sequencing the PCR product.

gene	t.test	tvalue	df	FDR
g28_1	Student	2.174	4	0.143
g28_2	Student	1.441	4	0.251
g28_3	Student	2.901	4	0.079
g28_4	Student	5.613	4	0.026
g28_5	Student	-3.559	4	0.053
g28_6	Student	1.109	4	0.330
g28_7	Student	1.869	4	0.174
g28_8	Student	-5.334	4	0.026
g28_9/10	Welch	-10.690	4	0.026

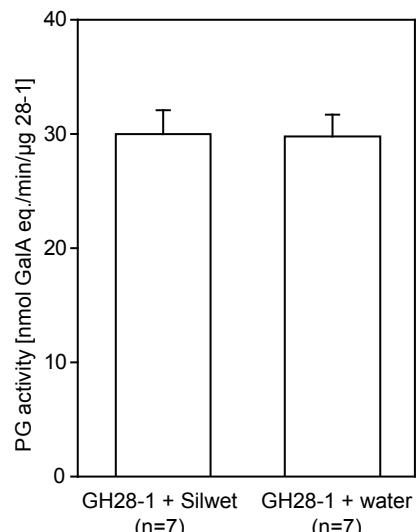
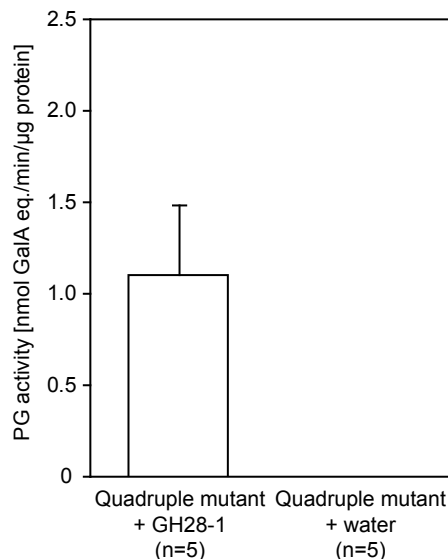
A**B**

Figure S7 Preliminary test in the context of the rescue experiment shown in Figure 4.

Quantification of PG activity of the (A) heterologously expressed GH28 protein with and without Silwet, the detergent reducing the surface tension of aqueous solutions, which was needed to impregnate leaves with GH28 protein ($P = 0.020$; t-test, $t = 2.899$) and of the (B) gut content of quadruple mutant larvae after overnight feeding on either leaves with or without GH28-1.

Table S1:

primer name	primer sequence	usage
FAM-M13(-20)F	gtaaaacgacggccagt	FAM labeled forward primer to 5' label GH28 diagnostic PCR amplicons for IDAA
PCO_GH28-1E3F	gtaaaacgacggccagtCGACATCAACACCACAGATCAAC	sequencing 28-1 exon3 & IDAA, forward primer (lower case is M13(-20) extension)
PCO_GH28-1E3R	caggaaacagctatgaccCTTCCATGGCAATGTTAC	sequencing 28-1 exon3, reverse primer (lower case is M13(-48mod) extension)
PCO_GH28-1E3R_short	CTTCCATGGCAATGTTACTG	IDAA 28-1 exon3, reverse primer
PCO_GH28-5E1F	gtaaaacgacggccagtTCTCTGTCAAACCTCGTAAC	sequencing 28-5 exon1 & IDAA, forward primer (lower case is M13(-20) extension)
PCO_GH28-5E1R	caggaaacagctatgaccTACCGCTGATCTGGATC	sequencing 28-5 exon1, reverse primer (lower case is M13(-48mod) extension)
PCO_GH28-5E1R_short	TACCGCTGATCTGGATC	IDAA 28-5 exon1, reverse primer
PCO_GH28-5E3Fnew	gtaaaacgacggccagtTCTCCTCCAGGCCACGAC	sequencing 28-5 exon3 & IDAA, forward primer (lower case is M13(-20) extension)
PCO_GH28-5E3R	caggaaacagctatgaccTTGATGACTCCGGACC	sequencing 28-5 exon3, reverse primer (lower case is M13(-48mod) extension)
PCO_GH28-5E3R_short	TTGATGACTCCGGACC	IDAA 28-5 exon3, reverse primer
PCO_GH28-9E1F	gtaaaacgacggccagtGTTCTCCGTCAAACTAGC	sequencing 28-9 exon1 & IDAA, forward primer (lower case is M13(-20) extension)
PCO_GH28-9E1R	caggaaacagctatgaccCATCCCAATGCGCAACTC	sequencing 28-9 exon1, reverse primer (lower case is M13(-48mod) extension)
PCO_GH28-9E1R_short	CATCCAATGCGCAACTC	IDAA 28-9 exon1, reverse primer
PCO_GH28-9E3Fnew	gtaaaacgacggccagtATCCTCCACCAGCAATGTC	sequencing 28-9 exon3 & IDAA, forward primer (lower case is M13(-20) extension)
PCO_GH28-9E3R	caggaaacagctatgaccCGATGACTCCAGGTCTC	sequencing 28-9 exon3, reverse primer (lower case is M13(-48mod) extension)
PCO_GH28-9E3R_short	CGATGACTCCAGGTCTC	IDAA 28-9 exon3, reverse primer
PCO_Fwd_28-9_10E3	TCCTCCACCAGCAATGTCGTATCTCTAAC	Identification of haplotype frequency (28-9 and 28-10) and (28-9) in wildtype
PCO_Rev_28-9_10E4	TGGAGTTCTTCCGGTCATGATCCGGACAC	Identification of haplotype frequency (28-9 and 28-10) and (28-9) in wildtype
crRNA name	crRNA target site sequence	usage
28-1E3a-sgRNA	TTAACAAATTGGATTGTTCcgg	knockout 28-1
28-1E3b-sgRNA	CATGGTTGAGTCTGTCAGTtgg	knockout 28-1
28-1E3c-sgRNA	ATCAAAACACATACCAATTCCcg	knockout 28-1
28-5/9E1-sgRNA	AGCTGCACCATCACCAAGCTTcg	knockout 28-5 & 28-9
28-5/9E3a-sgRNA	CTGCAGTGCTCAGGCGGCCAcgg	knockout 28-5 & 28-9
28-5/9E3b-sgRNA	GGGCATGAGCAAAACGTCCAaag	knockout 28-5 & 28-9